

Thermodynamic Performance Of A Co2 Vortex Tube Based On Cfd Flow Analysis

Kavitha K , Venkatachalam M.

Government college of Engineering , Salem- 11 , Anna University, Tamilnadu, India.
Corresponding author: Kavitha K

Date of Submission: 30-08-2020

Date of Acceptance: 08-09-2020

ABSTRACT - The vortex tube (VT) is a mechanical device that can simultaneously provide hot gas & cold air at extreme ends of the tube using compressed gas supplied at high pressure. In this work, a 3D CFD model is first developed to simulate the flow of CO₂ within a vortex tube, and then it is validated with published experimental data. The assumed k- ϵ turbulence model uses Tetra hedron elements generated in ANSYS Meshing. The validated CFD model is combined with a thermodynamic model of the VT to complete a parametric study, where the inlet pressure (550kPa to 1300kPa) and cold mass fraction (0.2 to 0.9) are the chosen parameters. The effects on the VT energy separation and performance are presented. Energy separation is discussed in terms of the hot exit and cold exit temperature differences, both with respect to the VT inlet temperature. Performance is characterized by cooling power, heating power, and both energy and exergy metrics. The numerical results show that the variation of the cold mass fraction from 0.2 to 0.9, for a fixed inlet pressure of 1300 kPa, causes the hot exit temperature difference to rise from 10 °C to 78.9 °C, while the cold exit temperature difference falls from 44.56°C to 17.15°C.

Keywords: Vortex tube, CO₂, CFD, exergy efficiency

I. INTRODUCTION

Refrigeration plays an important role in industry; hence researchers are looking for new techniques to enhance the efficiency of the systems that require refrigeration. With the rise in global population, industrialization, and growing worldwide energy consumption, there is a growing interest in the reuse of waste energy. Likewise, there is continuing interest in energy efficiency, as small change in efficiency can have a great impact on energy saving, particularly in devices that are not considered very efficient, such as the vortex tube. The vortex tube was discovered by the French scientist Raquel in 1931 and since then there have

been many research works on the performance of vortex tubes. A vortex tube is a device, which simultaneously produces both hot and cold streams from highly compressed gas. Fig. 1 shows the main parts and a schematic working of the vortex tube. Main parts of the vortex tube include cylinder, inlet nozzle diaphragm. Compressed air or other fluids is injected through the inlet nozzle tangentially and starts to swirl along the vortex tube. Two streams separately exit the vortex tube. The hot stream, which has a temperature higher than the inlet fluid, swirls peripherally and exits through a cone valve. The cold stream, which has a temperature lower than the inlet fluid, swirls in the center of the vortex tube and exits through a cold diaphragm. Stream, which has a temperature lower than the inlet fluid, swirls in the center of the vortex tube and exits through a cold diaphragm. Even though, it has been nine decades since the invention of the vortex tube, the concept of energy separation phenomena in the vortex tube is not well understood. Experiment and numerical studies have considered a variety of parameters while investigating the energy separation in the vortex tube.

II. EXPERIMENTATION

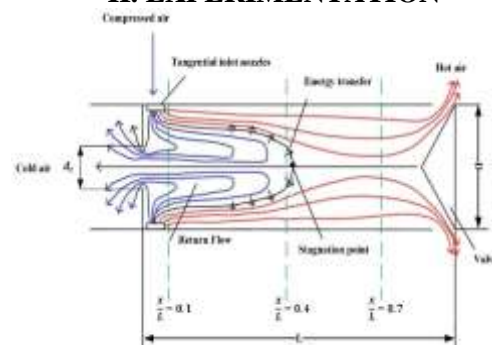


Figure.1. Flow pattern and schematic diagram of vortex tube

State of art:

Hirsch observed that compressed air at 6 atm and 20 °C produce 82 °C a temperature difference between the cold and hot exits ($\Delta T_{hc} = T_h - T_c$) due to internal friction between stream layers, and established a constant angular velocity between layers. Alborg and Groves carried out an experiment to measure the axial and angular velocities in the vortex tube. They observed that the amount of mass flow rate, which escapes at the cold exit, is less than amount of mass flow rate, which moves back toward the cold exit, which suggested that there is a secondary flow inside the vortex tube.

Ahbornetal proposed a new idea, whereby the secondary circulation acts as a heat pump which transfers energy from inner layer (near the core) to the outer layer (near the wall). Some numerical research illustrated that the secondary circulation depends on the ratio of cold the part diameter to tube diameter. Hundreds of experimental papers used air as a working gas and investigated different initial condition such as an inlet pressure, cold mass fraction and different vortex tube geometry. According to their results, with the increasing length of the vortex tube, as long as the stagnation point occurs inside the tube, temperature difference increases. An increase in the tube diameter has both an advantage and a disadvantage. On one hand, the angular velocity decreases and leads to lower centrifugal force and finally lower energy separation.

Guitar carried out an experiment with high pressure natural gas (78 and 88 bar). Based on their experiment, it was concluded that increasing the inlet pressure induces a higher velocity inside the tube, leading in turn to higher energy separation.

Xuetal used a large vortex tube, with a 2000 mm length and 60 mm diameter. They observed the transferring the forced vortex (swirl velocity is directly proportional to the radius ($V \propto r$)) near centerline to free vortex (swirl velocity is inversely proportional to the radius ($V \propto 1/r$)) at the hot exit near the wall because of decreasing the swirling velocity.

Aljuwayheletal investigated the energy separation inside the vortex tube with 2D axis symmetric CFD model and the results showed that work transfer due to torque produced by viscous shear can explain the energy separation.

Kirmac carried out an experimental investigation on air and oxygen and investigated the effect of number of inlet nozzle and inlet pressure. The results showed that increasing the number of nozzle leads to decrease the temperature

difference and the temperature difference increases due to increasing the inlet pressure.

Hanetal used R728, R744, R32, R22, R161, and R134a as working gases. The initial parameters were an inlet pressure from 0.2 to 1.3 and temperature was 12°C. They proposed that specific heat ratio, kinematic viscosity and thermal conductivity have an important influence on energy separation of the vortex tube; they also illustrated that the isentropic throttling effect on the cold exit of the working gas has a major impact on temperature difference between inlet and cold exit (ΔT_c). Their results showed that carbon dioxide has the highest temperature difference in comparison to air and nitrogen. A disadvantage of the experimental approach is the fact that applying some tools, such as a pitot tube to measure the velocity and other turbulent flow characteristics, might interrupt the highly turbulent flow pattern inside the vortex tube. This is why computational fluid dynamic (CFD) modeling helps to understand the flow characteristics.

Thakare and Parek employed the 2D CFD modeling with the standard turbulence model for a range of inlet pressures (2-5bar) in both non-isolated and isolated vortex tube. Their results showed that temperature difference is higher for isolated than non-isolated vortex tube. Also, they analyzed the temperature difference for four different working gases (air, N₂, O₂ and CO₂) and their results showed that has the highest and has the lowest energy separation. No validation with experimental data for N₂, O₂ and CO₂ was presented. Rafiee 3D modeling of a vortex tube with 6 inlet nozzles, using the standard turbulence model. Thakare and Parek studied the vortex tube with as the working gas, where the inlet temperature and total mass flow were fixed at 294.2 K and 8.35. The achieved results, however, are in contrast with each other for instance where $\alpha = 3$, with calculated cold exit temperatures of 246.48 K and 264.2 K, respectively. Farouk and Farouk compared $k-\epsilon$ and the large eddy simulation model predictions, it was found that the temperature separations predicted by the LES model was closer to the experimental results.

Aghagolietal used vortex tube in the Transcritical heat pump system instead of the expansion valve to partially recover the throttling losses and improve the heat pump cycle performance and the results showed that by partially replacing the vortex tube, the coefficient of the performance was improved by 8%. In the present study, a 3D simulation of the vortex tube is carried out using ANSYS FLUENT 18, and CO₂ is chosen as a working gas.

The modeling results are validated against the experimental data. Energy separation is discussed in terms of the hot exit and cold exit temperature differences, both with respect to the VT inlet temperature. Performance is characterized by cooling power, heating power, and both energy and exergy metrics.

Hanet shows R728, R744, R32, R22, R161, and R134a as working gases. The initial parameters were an inlet pressure from 0.2 to 1.3 and temperature was 12°C. They proposed that specific heat ratio, kinematic viscosity and thermal conductivity have an important influence on energy separation of the vortex tube; they also illustrated that the isentropic throttling effect on the cold exit of the working gas has a major impact on temperature difference between inlet and cold exit. In the present study, a 3D simulation of the vortex tube is carried out using ANSYS FLUENT 18, and CO₂ is chosen as a working gas.

The modeling results are validated against the experimental data. Energy separation is discussed in terms of the hot exit and cold exit temperature differences, both with respect to the VT inlet temperature. Performance is characterized by cooling power, heating power, and both energy and exergy metrics.

Governing equations of CFD modeling

In this study, a three-dimensional numerical model of the vortex tube has been developed using the standard $k-\epsilon$ turbulence model and flow pattern. In the vortex tube can be regarded as in steady state which $\partial p / \partial t = 0$.

The mass, momentum and energy equations for compressible turbulent flow in the vortex tube are:

$$\partial \rho / \partial t + \partial (\rho u) / \partial x + \partial (\rho v) / \partial y + \partial (\rho w) / \partial z = 0 \quad (1)$$

$$\rho \left(\frac{\partial u}{\partial t} + u \frac{\partial u}{\partial x} + v \frac{\partial u}{\partial y} + w \frac{\partial u}{\partial z} \right) = -\frac{\partial p}{\partial x} + \mu \left(\frac{\partial^2 u}{\partial x^2} + \frac{\partial^2 u}{\partial y^2} + \frac{\partial^2 u}{\partial z^2} \right) + \rho \beta g_x \quad (2)$$

$$\rho \left(\frac{\partial T}{\partial t} + u \frac{\partial T}{\partial x} + v \frac{\partial T}{\partial y} + w \frac{\partial T}{\partial z} \right) = \frac{\partial}{\partial x} \left(k \frac{\partial T}{\partial x} \right) + \frac{\partial}{\partial y} \left(k \frac{\partial T}{\partial y} \right) + \frac{\partial}{\partial z} \left(k \frac{\partial T}{\partial z} \right) + \rho \beta g_T \quad (3)$$

Following the recommendations of turbulence model is chosen for this study.

The standard $k-\epsilon$ model falls into the two equation turbulence category, which is based on transport equations for the turbulence kinetic energy (k) and its dissipation rate (ϵ). Transport equations for the standard model are as follow:

$$\frac{\partial k}{\partial t} + \frac{\partial (k u)}{\partial x} + \frac{\partial (k v)}{\partial y} + \frac{\partial (k w)}{\partial z} = G_k + G_b - \rho \epsilon - Y_M + S_k \quad (4)$$

$$\frac{\partial \epsilon}{\partial t} + \frac{\partial (\epsilon u)}{\partial x} + \frac{\partial (\epsilon v)}{\partial y} + \frac{\partial (\epsilon w)}{\partial z} = C_{1\epsilon} \frac{k}{l} \epsilon - C_{2\epsilon} \frac{\epsilon^2}{k} + S_\epsilon \quad (5)$$

G_b : The generation of turbulence kinetic energy because of buoyancy

Y_M : Contribution of the fluctuating dilatation in compressible turbulence to the overall dissipation rate

$\partial \epsilon / \partial k$: The turbulent Prandtl numbers for and respectively

S_k & S_ϵ : User-defined source terms

Boundary Condition

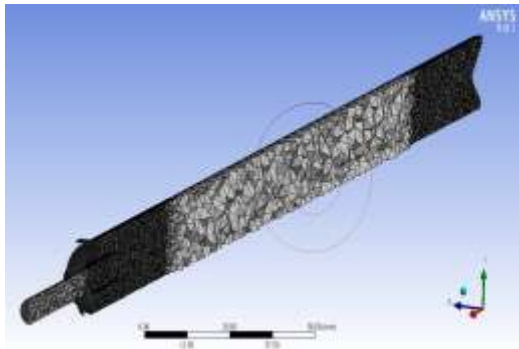
Geometry of Vortex tube used is shown in figure. In the this study, vortex tube inlet is given through 6 nozzles with a hot length of 300mm, tube diameter of 20mm thickness 1.5 mm and cold diameter of 6mm. In the current CFD modeling the exact model is simulated. The experimental pressures at the nozzle inlet, hot exit and cold exit are applied directly to the CFD model. The inlet of vortex tube has been assigned the boundary condition of pressure inlet which we have provided the values of pressure and temperature as 550kPa to 1300kPa and 285K, respectively. The hot and cold exits are considered as a pressure outlet. The no slip condition is assumed for the vortex inner walls. The simulation is done using the Pressure based Solver with SIMPLE algorithm.

All simulations are based on the Second Order Upwind scheme. The vortex tube model is designed in Solid Works for designing and drafting. CFD Modelling is done using the Solid Works model and fluid region is generated using ANSYS Design Modeler. Tetra mesh is generated using ANSYS Meshing; the simulation is carried out in ANSYS FLUENT. Adiabatic boundary condition for the walls, pressure outlet boundary condition for the cold and hot exits and pressure inlet The vortex tube model is designed in Solid Works for designing and drafting. CFD Modelling is done using the Solid Works model and fluid Where:

G_k : The generation of turbulence kinetic energy due to the mean velocity gradients region is generated using ANSYS Design Modeler. Tetra mesh is generated using ANSYS Meshing; the simulation is carried out in ANSYS FLUENT. Adiabatic boundary condition for the walls, pressure outlet boundary condition for the cold and hot exits and pressure inlet for the nozzle are considered.

Mesh

The 3D CFD mesh grid around the nozzle inlet, cold exit, and hot exit is shown in Fig. 3. In this model a tetra mesh is used. With respect to sizing of mesh, on sphere of radius option is used. By using this turbulence is capture more accurate at the inlet side along with the Cold outlet side and hot outlet side. Thus typical areas are captured accurately.



Mesh

Grid Independency

Grid independency is important to determine the optimum mesh number, meaning that the solution is independent of the mesh resolution. Therefore, 3D CFD analysis was carried out using different mesh sizes, with 1187994, 1560230 and 2076194 cells. It found that the percentage of cold temperature difference at 1560230 and 2076194 cells are less than 0.5%. Therefore, the 1560230 cell grid is chosen for the simulation. Increasing the number of cells more than 1560230 does not have a significant impact on the results.

THERMODYNAMIC MODEL OF VORTEX

The performance of the vortex tube relies on three main parameters: cold mass fraction, temperature difference, and hot exit temperature difference which are extracted from CFD results. The exergy efficiency will be applied to evaluate the vortex tube thermodynamic performance due to specific temperature differences, given some nominal information about the vortex tube. In the context of improving worldwide energy efficiency, it is important to analyze the performance of the vortex tube, which has not been considered in many research papers. The cold mass fraction will be varied from 0 to 1 ($0 \leq a \leq 1$) and defines as the ratio of the mass flow rate that is exhausted at the cold exit to the inlet mass flow rate. .

$$a = \frac{m_{cmin}}{m_{in}}$$

Cold and hot exit temperature difference

The cold exit temperature difference is defined as the difference between the average temperature at the cold exit and inlet temperature

$\Delta T = T_c - T_{in}$, The hot exit temperature difference is defined as the difference between the average temperature at the hot exit and inlet temperature.

$\Delta T_h = T_h - T_{in}$, The first law of thermodynamics states that during an interaction between a system and its surroundings, the amount of energy that the system gains must be exactly equal to the amount of energy lost by the surroundings.

The first law of thermodynamics can be written as:

$$E = Q - W$$

E Represents the sum of thermal energy, kinetic energy and etc.

Applying the first law on the vortex tube,

$$m_{in} h_0 = m_c h_c + m_h h_h$$

Applying the second law of thermodynamics to the vortex tube with $Q = 0$

$$S_{in} - S_c - S_h - S_{irr} = 0$$

$$S_{irr} = m_c \ln \frac{T_c}{T_0} + m_h \ln \frac{T_h}{T_0}$$

$$S_{irr} = m_c \ln \frac{1-a}{T_0} + m_h \ln \frac{a}{T_0}$$

II. RESULTS AND DISCUSSION

In the present study, the effect of inlet pressure and cold mass fraction, which is varied by changing the pressure at the hot exit, are investigated on different aspects of vortex tube. Energy separation is discussed in terms of the hot exit and cold exit temperature differences, both with respect to the VT inlet temperature. Performance is characterized by cooling power, heating power, and both energy and exergy efficiencies. To better understanding the flow inside the vortex tube temperature, pressure, velocity in different sections of vortex tube and, the effect of inlet pressure and cold mass fraction are investigated on cooling and heating power, COP and exergy efficiency. Pressure contours, Temperature Contours and velocity contours of the tube is shown below.

Power capacity

Inlet pressure(Kpa)	Temp difference	Cold mass fraction	Cooling capacity
550	23.15	0.2	234.25
550	21.17	0.3	233.40
550	20.30	0.4	210.08
550	18.14	0.5	209.32
550	15.09	0.6	207.13
550	12.50	0.7	205.27
550	9.40	0.8	203.40
550	5.50	0.9	200.24

Table: 7 Cooling power and cold mass fraction

Inlet pressure(Kpa)	Temp difference	Cold mass fraction	Cooling capacity
850	32.50	0.2	219.65
850	30.25	0.3	216.03
850	27.17	0.4	215.82
850	24.32	0.5	213.77
850	23.14	0.6	211.46
850	21.11	0.7	209.29
850	18.09	0.8	205.06
850	9.34	0.9	203.00

Table: 8 Cooling power and cold mass fraction

Inlet pressure(Kpa)	Temp difference	Cold mass fraction	Cooling capacity
1300	32	0.2	223.32
1300	30.25	0.3	224.18
1300	27.17	0.4	219.11
1300	24.32	0.5	220.11
1300	23.14	0.6	219.43
1300	21.11	0.7	217.90
1300	18.09	0.8	213.65
1300	9.34	0.9	210.55

Table: 9 Cooling power and cold mass fraction

Inlet pressure(Kpa)	Temp difference	Cold mass fraction	Heating capacity
550	5.5	0.2	200.24
550	10.12	0.3	202.94
550	14.20	0.4	206.49
550	16.50	0.5	208.31
550	18.15	0.6	209.93
550	23.18	0.7	215.13
550	27.32	0.8	228.13
550	44.30	0.9	235.12

Table:10 Heating power and cold mass fraction

Inlet pressure(Kpa)	Temp difference	Cold mass fraction	Heating capacity
850	10.02	0.2	203.43
850	12.43	0.3	205.22
850	17.90	0.4	209.15
850	22.10	0.5	215.89
850	31.5	0.6	216.80
850	40.2	0.7	225.76
850	47.25	0.8	227.32
850	54.20	0.9	243.39

Table: 11 Heating power and cold mass fraction

Inlet pressure(Kpa)	Temp difference	Cold mass fraction	Heating capacity
1300	10.02	0.2	203.48
1300	15.09	0.3	207.13
1300	22.501	0.4	212.46
1300	32.65	0.5	219.76
1300	40.18	0.6	225.17
1300	42.11	0.7	226.56
1300	53.10	0.8	234.46
1300	78.18	0.9	246.74

Table: 12 Heating power and cold mass fraction

VI. CONCLUSION:

CFD analysis was conducted to illustrate the energy separation in the vortex tube with CO₂ as a real gas at the different inlet pressure and cold mass fraction. Energy separation was discussed in terms of the hot exit and cold exit temperature differences, both with respect to the vortex tube inlet temperature. Performance is characterized by cooling power, heating power, and both energy and exergy metrics. With increasing inlet pressure, the

cold exit temperature decreases while the hot exit temperature increases. Increasing the inlet pressure leads to increasing the magnitude of the velocity and increasing the vortex tube performance. The COP of the vortex tube was investigated when it is understood to acts as a heat pump and refrigeration. Even though, increasing the pressure causes the rising the cooling and heating power, and goes through the maximum. The maximum value for exergy efficiency depends on both heating and cooling power rates directly hence maximum value of either heating or cooling power rate at specific cold mass fraction is not concluded that maximum efficiency occurs at the same cold mass fraction.

REFERENCES

- [1]. P. Maina, Z. Huan, A review of carbon dioxide as a refrigerant in refrigeration technology, *S. Afr. J. Sci.* 111 (2015) 1–10. doi:10.17159/sajs.2015/20140258.
- [2]. K.D. Devade, A.T. Pise, Issues and prospects of energy separation in vortex tubes: Review, *Heat Transf. - Asian Res.* (2017) 1–31. doi:10.1002/hjt.21313.
- [3]. H.M. Skye, G.F. Nellis, S.A. Klein, Comparison of CFD analysis to empirical data in a commercial vortex tube, *Int. J. Refrig.* 29 (2006) 71–80. doi: 10.1016/j.ijrefrig.2005.05.004.
- [4]. T. Dutta, K.P. Sinhamahapatra, S.S. Bandyopadhyay, CFD Analysis of Energy Separation in Ranque-Hilsch Vortex Tube at Cryogenic Temperature, (2013). doi:10.1155/2013/562027.
- [5]. R. Hilsch, The use of the expansion of gases in a centrifugal field as cooling process, *Rev. Sci. Instrum.* 18 (1947) 108–113. doi:10.1063/1.1740893.
- [6]. B. Ahlborn, S. Groves, FLUID DYNAMICS Secondary flow in a vortex tube, *Fluid Dyn. Res.* 21 (1997) 73–86
- [7]. B.K. Ahlborn, J.U. Keller, E. Rebhan, The heat pump in a vortex tube, *J. Non-Equilibrium Thermodyn.* 23 (1998) 159–165. doi:10.1515/jnet.1998.23.2.159.
- [8]. U. Behera, P.J. Paul, S. Kasthuriangan, R. Karunanithi, S.N. Ram, K. Dinesh, S. Jacob, CFD analysis and experimental investigations towards optimizing the parameters of Ranque-Hilsch vortex tube, *Int. J. Heat Mass Transf.* 48 (2005) 1961–1973. doi:10.1016/j.ijheatmasstransfer.20.046.
- [9]. U. Behera, P.J. Paul, K. Dinesh, S. Jacob, Numerical investigations on flow behaviour and energy separation in Ranque-Hilsch vortex tube, *Int. J. Heat Mass Transf.* 51 (2008) 6077–6089. doi:10.1016/j.ijheatmasstransfer.2008.03.029.
- [10]. M.O. Hamdan, S.A.B. Al-Omari, A.S. Oweimer, Experimental study of vortex tube energy separation under different tube design, *Exp. Therm. Fluid Sci.* 91 (2018) 306311. doi:10.1016/j.expthermflusci.2017.10.03
- [11]. A.D. Gutak, Experimental investigation and industrial application of Ranque-Hilsch vortex tube, *Int. J. Refrig.* 49 (2015) 93–98. doi:10.1016/j.ijrefrig.2014.09.021.
- [12]. Y. Xue, M. Arjomandi, R. Kelso, Experimental study of the thermal separation in a vortex tube, *Exp. Therm. Fluid Sci.* 46 (2013) 175182. doi:10.1016/j.expthermflusci.2012.12.09
- [13]. N.F. Aljuwayhel, G.F. Nellis, S.A. Klein, Parametric and internal study of the vortex tube using a CFD model, *Int. J. Refrig.* 28 (2005) 442–450. doi:10.1016/j.ijrefrig.2004.04.004.
- [14]. K. Volkan, Exergy analysis and performance of a counter flow Ranque – Hilsch vortex tube having various nozzle numbers at different inlet pressures of oxygen and air, *32 (2009) 1626–1633.* doi:10.1016/j.ijrefrig.2009.04.007.
- [15]. X. Han, N. Li, K. Wu, Z. Wang, L. Tang, G. Chen, X. Xu, The influence of working gas characteristics on energy separation of vortex tube, *Appl. Therm. Eng.* 61 (2013) 171–177. doi:10.1016/j.applthermaleng.2013.07.027.
- [16]. N. Agrawal, S.S. Naik, Y.P. Gawale, Experimental investigation of vortex tube using natural substances, *Int. Commun. Heat Mass Transf.* 52 (2014) 51–55. doi:10.1016/j.icheatmasstransfer.2014.01.009.
- [17]. H.R. Thakare, A.D. Parekh, Experimental investigation & CFD analysis of Ranque-Hilsch vortex tube, *Energy.* 133 (2017) 284–298. doi:10.1016/j.energy.2017.05.070.
- [18]. H.R. Thakare, A.D. Parekh, Computational analysis of energy separation in counter-flow vortex tube, *Energy.* 85 (2015) 62–77. doi:10.1016/j.energy.2015.03.058.
- [19]. S.E. Rafiee, M.M. Sadeghiazad, Experimental and 3D CFD investigation on heat transfer and energy separation inside a counter flow vortex tube using different

- shapes of hot control valvesAppl. Therm. Eng. 110 (2017) 648–664. doi:10.1016/j.applthermaleng.2016.08.166.
- [20]. M.R. and A.H. N. Pourmahmoud, S.E Rafiee, Numerical Energy Separation analysis on the commercial Ranque-Hilsch vortex tube on basis of application of different gases, Sci. Iran. Trans. B Mech. Eng. 20 (2013) 1528–1537.